

Molecular Dynamics Simulations on the First Two Helices of Vpu from HIV-1

I. Sramala,* V. Lemaitre,*[†] J. D. Faraldo-Gómez,[‡] S. Vincent,[†] A. Watts,* and W. B. Fischer*

*Biomembrane Structure Unit, Department of Biochemistry, Oxford University, Oxford OX1 3QU, UK; [†]Nestlé Research Center, Bioscience Department, Vers-Chez-Les-Blanc, CH-1000 Lausanne 26, Switzerland; and [‡]Laboratory of Molecular Biophysics, Department of Biochemistry, Oxford University, Oxford OX1 3QU, UK

ABSTRACT Vpu is an 81 amino acid protein of HIV-1 with two phosphorylation sites. It consists of a short N-terminal end traversing the bilayer and a longer cytoplasmic part. The dual functional role of Vpu is attributed to these topological distinct regions of the protein. The first 52 amino acids of Vpu (HV1H2) have been simulated, which are thought to be embedded in a fully hydrated lipid bilayer and to consist of a transmembrane helix (helix-1) connected via a flexible linker region, including a Glu-Tyr-Arg (EYR) motif, with a second helix (helix-2) residing with its helix long axis on the bilayer surface. Repeated molecular dynamics simulations show that Glu-28 is involved in salt bridge formation with Lys-31 and Arg-34 establishing a kink between the two helices. Helix-2 remains in a helical conformation indicating its stability and function as a “peptide float,” separating helix-1 from the rest of the protein. This leads to the conclusion that Vpu consists of three functional modules: helix-1, helix-2, and the remaining residues toward the C-terminal end.

INTRODUCTION

Viral genomes encode for a series of short membrane proteins with an average length of ~100 amino acids (Cohen et al., 1988; Strebel et al., 1988). Most of these proteins fulfill their role to enable and/or improve the efficiency of viral replication (M2, NB, CM2, Vpu, and others) (Fischer and Sansom, 2002), whereas others are involved in the construction of, for example, protein shells to wrap the viral genome (Pf1, M13, and others). A common theme of all of these small proteins is that some of them have at least two functional roles and can therefore be seen as multifunctional tools.

Vpu is encoded in the genome of HIV-1 (Cohen et al., 1988; Strebel et al., 1988) together with accessory proteins, such as Vif, Vpr, and Nef. Vpu is found especially in the endoplasmic reticulum and is neither found in the virion nor in the cell membrane of the infected cell (Strebel et al., 1989). It has a dual role in the life cycle of HIV-1, which is i), to enhance viral particle release (Deora et al., 2000; Paul et al., 1998; Schubert et al., 1996a) and ii), to be involved in the degradation of the HIV-1 receptor protein CD4 (Bour et al., 1995; Schubert et al., 1996b; Strebel et al., 1989; Willey et al., 1992). Although it is found that for the latter role the cytoplasmic part of Vpu is responsible, enhanced particle release is thought to be due to channel activity initiated by the assembly of a few Vpu proteins, which is dependent on the transmembrane (TM) part (Ewart et al., 1996; Marassi et al., 1999; Schubert et al., 1996b). To sub-

stantiate this, mutations in the TM part show a lower rate of particle secretion (Tiganos et al., 1998).

There is a significant amount of structural information available for the 81 amino acid protein Vpu. This information is based on investigations of peptides analogous of Vpu, and full-length Vpu derived from NMR (Coadou et al., 2001; Federau et al., 1996; Henklein et al., 2000; Ma et al., 2002; Marassi et al., 1999; Willbold et al., 1997; Wray et al., 1995; Wray et al., 1999), CD- (Wray et al., 1995), and FTIR-spectroscopy (Kukol and Arkin, 1999). In summary, it has been concluded that Vpu has a short N-terminal extramembraneous end and a TM spanning helix that is tilted by ~10–20°. A loop connects the TM helix with a second helix (helix-2) that resides with its helix long axis parallel to the membrane surface. Another flexible part, including the two phosphorylation sites (Ser-52 and Ser-56), connects helix-2 with a third helix. Toward the C-terminal end another short helix (Federau et al., 1996) or a turn (Willbold et al., 1997) exists, depending on the conditions under which the data have been recorded.

Molecular dynamics (MD) simulations play an important role in linking structural information from experiments with the mechanisms of the protein on an atomic scale. Investigations on K⁺ channels may stand as one of the most comprehensive examples in this respect (reviewed in Sansom et al. (2002)). In the case of Vpu, MD simulations have dealt so far with the analysis of the TM part of Vpu (Cordes et al., 2001, 2002; Grice et al., 1997; Lopez et al., 2002; Moore et al., 1998). Up to six TM helices have been aligned in parallel to form an assembly of homooligomers embedded in a low-dielectric slab (Grice et al., 1997), an octane slab as a bilayer mimic (Lopez et al., 2002; Moore et al., 1998), and a fully hydrated lipid bilayer (Cordes et al., 2001, 2002; Lopez et al., 2002). All studies have in common a fairly good agreement with structural data from experiment. They also suggest that a pentameric bundle should be

Submitted August 17, 2002, and accepted for publication January 3, 2003.

Address reprint requests to W. B. Fischer, Tel.: +44-1865-275776; Fax: +44-1865-275234; E-mail: wolfgang.fischer@bioch.ox.ac.uk.

I. Sramala's present address is Institute of Molecular Biology and Genetics, Mahidol University, Salaya Campus, Nakornpathom, Thailand.

© 2003 by the Biophysical Society

0006-3495/03/05/3276/09 \$2.00

the minimum assembly for Vpu to form an ion-conducting pore (Cordes et al., 2002; Grice et al., 1997; Lopez et al., 2002).

In an earlier computational study the TM helix (helix-1) of Vpu embedded in a fully hydrated lipid bilayer (Fischer et al., 2000) has been investigated. In this study the focus is on an extended model Vpu₁₋₅₂ including helix-2 laying on top of the lipid membrane. It has been proposed that amino acids Glu-28, Tyr-29, and Arg-30 (EYR motif) play a key role in the bend of the strand. Up to now detailed structural data on this region are not available. Driven by the good agreement of the recent computational data with those from spectroscopy, the role of these particular amino acids on the stability of the protein solely based on the simulations can be proposed. MD simulations have been repeated to assess the reliability of the data acquisition (van Gunsteren and Mark, 1998). The data will be discussed against the background of computational investigations on other viral membrane proteins such as the Pf1 coat protein from filamentous bacteriophage (Milik and Skolnick, 1993; Roux and Woolf, 1996; Tobias et al., 1993), which adopt a similar kinked-like structure. In addition, the idea that Vpu protein consists of “functional modules” is addressed.

MATERIALS AND METHODS

A helical model of the first 52 amino acids of Vpu was generated, Vpu₁₋₅₂:



using a combined simulated annealing and molecular dynamics simulations (SA/MD) approach applying the program Xplor (Brünger, 1992). An extended description of the procedure is given in detail elsewhere (Kerr et al., 1994). The procedure is summarized in brief. The SA/MD protocol comprises two stages. In Stage 1 an idealized α -helix is constructed on the basis of the backbone $\text{C}\alpha$ -atoms of the peptide. All other atoms of the individual amino acids are superimposed on their particular $\text{C}\alpha$ -atoms. During Stage 1 the side-chain atoms “evolve” from the $\text{C}\alpha$ -atoms while retaining the $\text{C}\alpha$ -atoms in fixed positions. Beginning the annealing at 1000 K, the weights for bond length, bond angles, planarity, and chirality are gradually increased. A repulsive van der Waals term is slowly introduced after an initial delay of up to 80% of the original values. This allows the atoms to pass each other. Five structures for each helix were obtained. Each helix from Stage 1 is used for five molecular dynamics runs in Stage 2. In Stage 2, initial velocities correspond to 500 K. Harmonic restraints hold the $\text{C}\alpha$ -atoms, but are relaxed as the temperature drops from 500 to 300 K. At this stage distance restraints are introduced and the $\text{C}\alpha$ -atoms are allowed to move. In Stage 2 electrostatic interactions are introduced into the potential energy function. The main-chain atoms obtain their charges corresponding to the PARAM19 parameter set. Partial charges on side-chain atoms of polar side chains are gradually scaled up (from 0.05 to 0.4 times their full value) during the temperature reduction from 500 to 300 K. The scaling factor 0.4 is also applied during the 5-ps dynamics and energy minimization. A distance-dependent dielectric function is used (Brünger, 1992), with a switching function smoothly truncating distant electrostatic interactions. In Stage 2, $5 \times 5 = 25$ helices are obtained and the most straight helix is used to run the simulations.

The chosen helix was manually bent around residues Glu-28 to Ile-32 using the program Swiss PDB-Viewer to adopt the helix-loop-helix motif.

The ϕ - and ψ -values (ϕ/ψ in $^\circ$) were intended to be held in a helical conformation: Glu-28: $-70.4/0.2$; Tyr-29: $-65.2/-42.5$; Arg-30: $-84.7/-13.8$; Lys-31: $-86.2/10.0$; Ile-32: $-57.6/-18.0$ (all values after the bend). This procedure allowed the $\text{C}\alpha$ -atom of residue Asp-39 to point toward the bilayer surface and the $\text{C}\alpha$ -atom of residue Arg-48 to point away from the surface (see also Henklein et al. (2000)).

A hole in a lipid bilayer consisting of 288 POPC (1-palmitoyl-2-oleoyl-*sn*-glycerol-3-phosphatidyl-choline) molecules was created by overlaying a bent peptide model with the lipid bilayer, which was derived from GRASP software. Lipid molecules for which the phosphorous atoms were overlapping with the GRASP representation of the peptide were removed (Faraldo-Gómez et al., 2002). This leads to a removal of an unequal number of lipids on both sides of the bilayer resulting in 125 lipids in the leaflet with helix-2 and 136 lipids in the other leaflet (261 lipids in total) with 13,572 lipid atoms. After insertion of Vpu₁₋₅₂ (529 peptide atoms) the peptide/lipid system (Fig. 1 A) was hydrated with 16,169 water molecules (48,507 water atoms). The overall number of atoms in the simulation at this stage is 62,610, including two Cl^- ions to neutralize the simulation box. To allow the lipid molecules next to helix-2 to fill the “hole” beneath it, 600 ps of equilibration at 300 K with the protein restrained is performed (Fig. 1 B). Thereby the peptide coordinates were restrained. The production phase was run at 300 K for up to 9 ns and twice up to 3 ns, each starting with randomly chosen initial velocities.

Gromacs 2.0 and 3.0 software (<http://www.gromacs.org>) was used including the simple point charge (SPC) water model (Berendsen et al., 1987). Simulations were run on either a VALinux Beowulf cluster of four dual Pentium III 700-Mhz processors or a Dell OptiPlex GX1 with a Pentium III 450-MHz processor. The simulations used a time step of 2 fs and a LINCS algorithm to keep the geometry of the molecules. An isothermal-isobaric ensemble (NPT) was used with periodic boundaries and anisotropic pressure coupling (Gromacs 2.0) or Berendsen temperature and pressure coupling (Gromacs 3.0). Long-range electrostatics have been calculated with the particle-mesh Ewald (PME) method. Lennard-Jones and short-range Coulombic interactions were cut off at 1.0 and 0.9 nm, respectively.

RESULTS

The evolution of the adaptation of Vpu₁₋₅₂ to the lipid membrane environment is shown in Fig. 1 A. At the beginning, the TM helix (helix-1) and helix-2 spanning an angle of $\sim 100^\circ$ with the helix normal of helix-2 almost parallel to the membrane surface. In this configuration, Ser-23 is not buried under helix-2. Helix-2 resides on top of the lipid headgroup region (*gray spheres* in Fig. 1 A). The snapshots taken at 3 and 6 ns imply a wavelike motion of Vpu₁₋₅₂ being partially ejected from the bilayer and driven back into it. At 9 ns helix-2 is found to be embedded in the lipid headgroup region, as would be expected for its partially hydrophobic character along the membrane-facing side of the helix. Helix-1 adopts a considerable kink in certain time steps. Throughout the simulation the lipids remain fairly packed beneath helix-2 (Fig. 1 B) allowing the hydrophobic part of the lipid molecules to be in contact with the bilayer facing hydrophobic side of helix-2. The lipid headgroups do not maneuver underneath helix-2 but rather stay away from helix-2.

The root mean square deviation (RMSD) for the $\text{C}\alpha$ -atoms for the simulation over 9 ns levels off after ~ 0.5 ns reaching values between 0.2 and 0.25 nm (*black trace* in Fig. 2). The

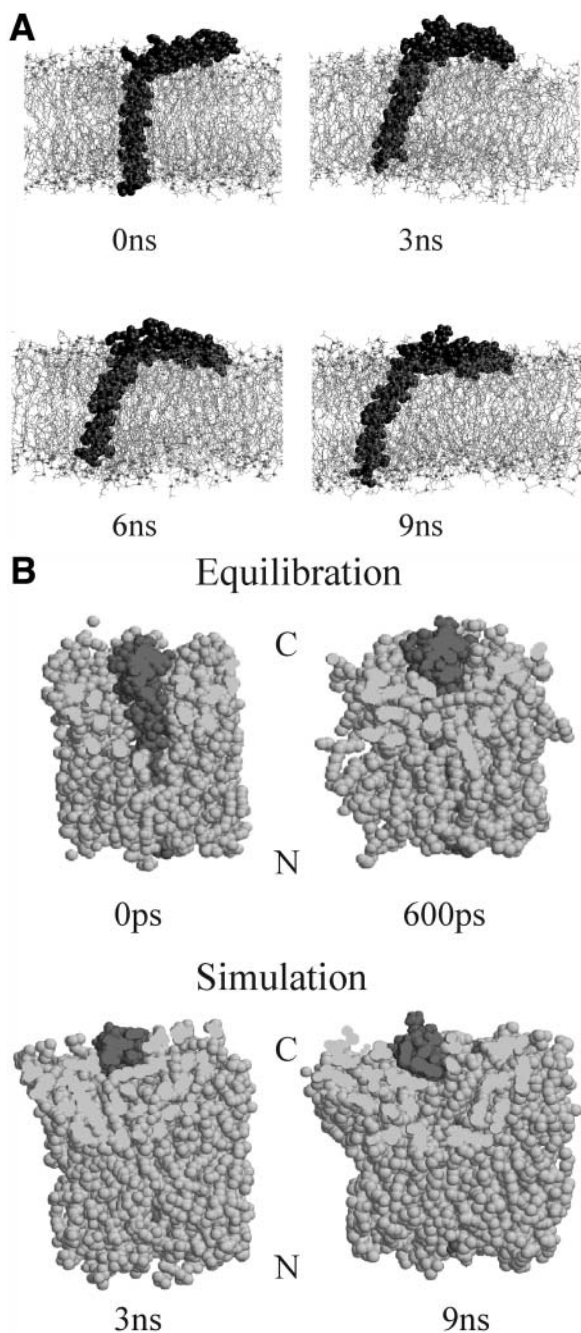


FIGURE 1 Snapshots of the protein (*black*) embedded in a lipid bilayer (*thin gray chains, gray spheres* represent the phosphorous headgroups) at 0, 3, 6, and 9 ns (*A*). View from the C- to the N-terminal end of Vpu along the axis of helix-2 (*dark*) lying on top of the bilayer (*gray*) before (0 ps) and after 600 ps of equilibration with the protein (*dark*) restraint (*B*). Snapshots taken from the simulations at 3 ns and 0 ns are shown in the lower half. The figures are created with the software Rasmol in the slab mode showing the atoms with their van der Waals radii. Plain gray spots are sliced atoms due to the slab-mode representation.

trace shows three maxima at around 2.5, 5, and 6 ns. Values for a second and third run over 3 ns behave in a similar way, leveling off after ~ 0.5 ns but at slightly higher and lower values (*gray traces* in Fig. 2) compared to the run over 9 ns.

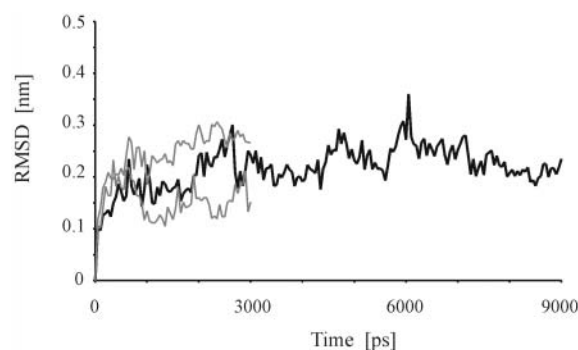


FIGURE 2 Root mean square deviation (RMSD) of the $C\alpha$ -atoms of the simulation over 9 ns (*black trace, thick line*) and two simulations each over 3 ns (*gray and black thin lines*).

The interconnecting region of the two helices is highlighted in Fig. 3. At the beginning of the simulation Asp-39 is pointing toward the hydrophobic region of the bilayer, whereas Arg-44 stretches into the aqueous environment (Fig. 3 *A*). After 3 ns both residues reverse their position with Asp-39 now facing the aqueous phase and Arg-44 the lipid bilayer. This revolution is accompanied by the unwinding of parts of the region interconnecting the two helices (Fig. 3 *B*). Although residues Glu-28 (*light gray*, Fig. 3 *B*) and Tyr-29 (*gray*, Fig. 3 *B*) remain within a helical conformation of the backbone, Arg-30 (*black*, Fig. 3 *B*) and Lys-31 (*black*, Fig. 3 *B*) seem to be involved in the unwinding process. Arg-34 (*light gray*, Fig. 3 *B*) is back in a helical conformation. A more thorough analysis of the ϕ and ψ values of these residues indicate that Glu-28 and Tyr-29 do not deviate from standard values for helices (Branden and Tooze, 1991) during the entire duration of the 9-ns simulation (Fig. 4). Arg-30 is involved in the unwinding process because its ϕ and ψ values undergo large deviations especially within the first half of the simulation. The values for Lys-31 rapidly adopt values of around -100° for ϕ and $\sim 150^\circ$ for ψ within the first 200 ps. The ϕ and ψ values for Ile-32 fluctuated around $\sim -100^\circ$ (for ϕ) and -50° (for ψ) and Leu-33 returned almost completely to a helical conformation. Averaged data for 0, 3, and 9 ns are given in Table 1. In the second and third run (both 3 ns) all traces match those shown in Fig. 4 for the first 3 ns. At the C- and the N-terminal end no significant unwinding of the helices is observed.

The helical environment around Glu-28 to Arg-30 is supported by a salt bridge between Glu-28 and Lys-31, shown in Fig. 3 *B*, with a distance of around 0.15 nm during the entire duration of the 9-ns simulation (*black trace* in Fig. 5). Arg-34 also forms a salt bridge with Glu-28 (*gray trace* in Fig. 5) after 2 ns forming a “complex salt bridge” (Musafia et al., 1995). In repeated simulations, the salt bridge between Glu-28 and Lys-31 undergoes a more rapid adaptation of an average distance of 0.15 nm compared to the salt bridge formation by Glu-28 with Arg-34 (Fig. 5, *B* and *C*). It seems that the formation of the salt bridge between

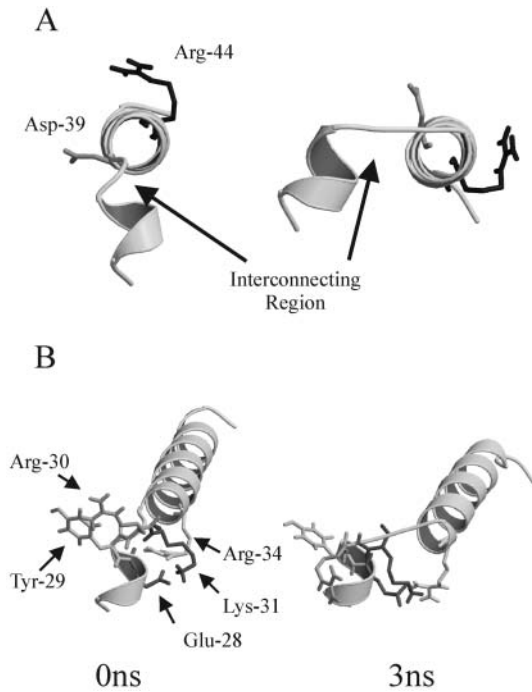


FIGURE 3 View from the N- to the C-terminal end of helix-2 along its long axis (A). Highlighted are residues Asp-39 (gray) and Arg-44 (black). View from top onto the kink between helix-1 and helix-2 (B). Residues shown are Glu-28 (light gray), Tyr-29 (gray), Arg-30 (black), Arg-34 (light gray). In both panels lipids and water molecules are omitted for clarity. For data representation the Molscript software is used.

Glu-28 and Arg-34 triggers or at least supports the revolution of helix-2, as mentioned, accompanied with the unwinding of the helical structure between Arg-30 and Ile-32.

As a result, Glu-28 and Tyr-29 are unlikely to be the key residues forming the bend between helix-1 and helix-2. Arg-30 is not in a helical conformation for short time steps during the simulation, which supports earlier findings (Cordes et al., 2002) in that it is most likely fulfilling its role as a flexible residue. However, Lys-31 and Ile-32 seem to be involved in forming the kink, because they are largely diverting from the normal values for an ideal helix over the entire duration of the simulation.

There is a sequence of alternating negatively and positively charged residues in Vpu: Asp-39, Arg-40, Asp-43, Arg-44, Glu-47, Arg-48, Asp-51, which forms another “complex salt bridge” (data not shown). The sequence is held together within distances of less than 0.2 nm between each of the residues. Because two hydrophobic residues separate each of the DR/ER repeats (3.6 residues per turn for an ideal helix) the hydrophilic residues involved in the salt bridge perform a slightly left-handed twist. The complex salt bridge is a combination of (i,i+1)D/E,R and (i,i+3)R,D/E motives. This is different from the (i,i+4)E,K motif, which has been found to promote helix conformation (Marqusee and Baldwin, 1987). The fact that the salt bridge is not buried (Hensch and Tidor, 1994; Horowitz et al., 1990; Wald-

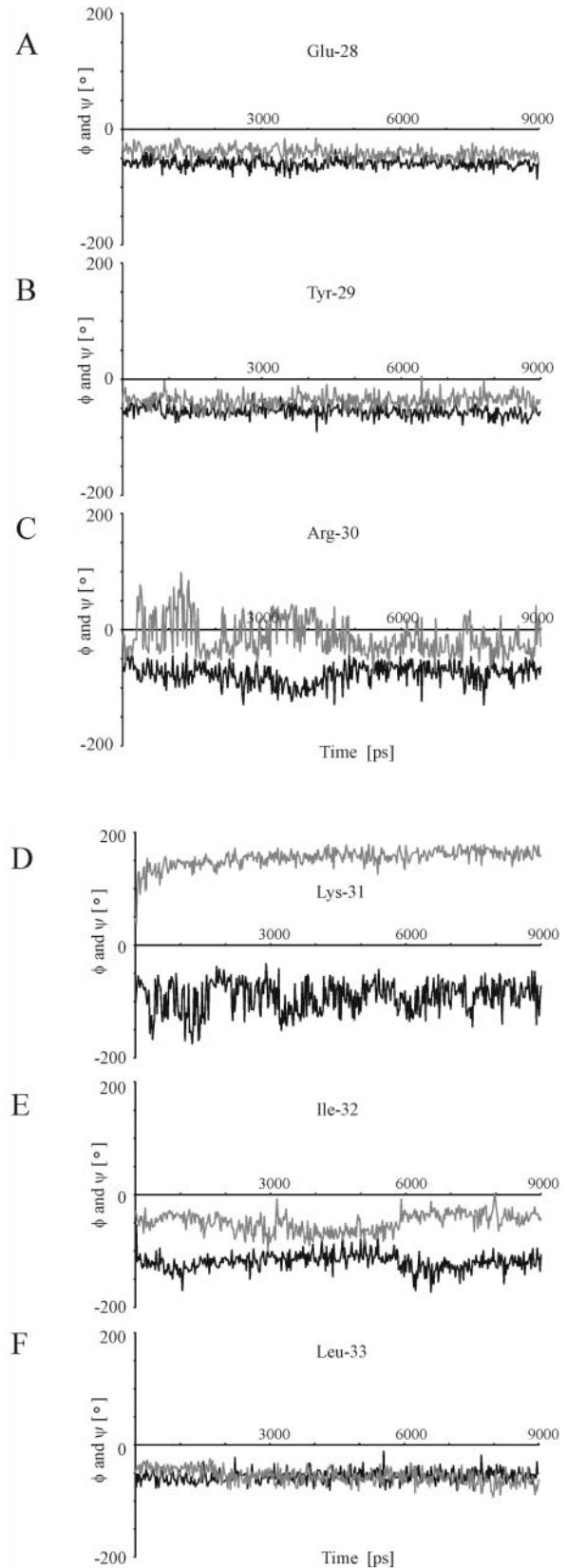


FIGURE 4 Time-dependent representation of the ϕ - (black traces) and ψ -values (gray traces) for the residues Glu-28 (A), Tyr-29 (B), Arg-30 (C), Lys-31 (D), Ile-32 (E), and Leu-33 (F).

TABLE 1 Simulated structural data of Vpu₁₋₅₂

Runs	Helix-1				Helix-2				
	1st	2nd	3rd	Average	1st	2nd	3rd	Average	
Tilt angle [°]	0 ns	4.3 (3.8)	8.6 (3.6)	7.0 (3.2)	6.6 (3.8)	7.5 (2.1)	-2.3 (4.8)	4.3 (2.3)	3.1 (5.2)
	3 ns	16.3 (2.3)	21.1 (1.7)	18.0 (1.9)	18.5 (2.8)	-15.4 (2.0)	-4.3 (1.5)	2.3 (3.1)	-5.8 (7.8)
	9 ns	23.3 (2.1)	-	-	-	-10.2 (2.0)	-	-	-
Kink angle [°]	0 ns	5.8 (3.8)	13.0 (1.2)	8.6 (4.3)	9.1 (4.4)	4.8 (3.2)	13.0 (1.5)	3.1 (1.5)	6.9 (4.9)
	3 ns	7.1 (2.9)	15.4 (1.3)	4.2 (1.6)	8.9 (5.3)	13.0 (3.3)	11.0 (0.7)	2.6 (0.5)	8.9 (5.0)
	9 ns	7.2 (2.6)	-	-	-	-	7.0 (3.9)	-	-

Data results from an average of five data sets recorded at 0–400, 2600–3000, and 8600–9000 ps in steps of 100 ps including the standard deviation shown in brackets. The average values derive from 15 data sets in the particular time frame and their standard deviation. For the 2nd and 3rd runs data are only available up to 3 ns.

burger et al., 1995) and the negatively charged residue starts at the amino terminal end (Marqusee and Baldwin, 1987), suggests that the motif has a stabilizing effect on the helical conformation.

After 0.5 ns of simulation, helix-1 approaches an average tilt angle of $\sim(23.3 \pm 2.1)^\circ$ (Table 1 and *black trace* in Fig. 6 A). Helix-2 penetrates with its C-terminal end into the lipid

bilayer confining an average angle of its helix long axis with the plane of the bilayer at $\sim(10.2 \pm 2.0)^\circ$. This final conformation is reached within the first 3 ns (*gray trace* in Fig. 6 A). The resulting angle between these two helices is shown in Fig. 6 B. During the simulation the angle between the two helices oscillates between 90 and 100°. Helix-1 is seen to be considerably kinked $\sim(7.2 \pm 2.6)^\circ$ with occasionally larger values of up to 15°. The latter value is still lower than the angle of $\sim 25^\circ$ found for proline-induced kinked TM helices in membrane proteins (Barlow and Thornton, 1988; Boncheva and Vogel, 1997; Deisenhofer et al., 1985). Helix-2 adopts kink angles in the same range as helix-1 (Table 1). In Table 1 averaged values for the two repeated runs over 3 ns are listed. They show the spread ranging from 4 to 15° for both helices. The kink of helix-1 is in the same range as found for the same helix in an assembly of homooligomers forming a pore (Cordes et al., 2002). It is suggested that helix-2 lies along the membrane surface and is not an “ideal straight” helix.

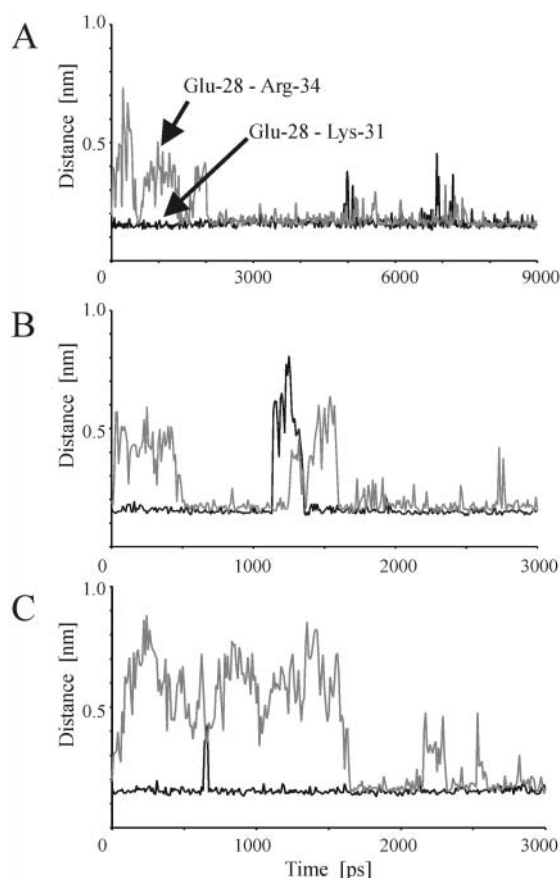


FIGURE 5 Time-dependent representation of the distances between Glu-28-Lys-32 (*black trace*) and Glu-28-Arg-34 (*gray trace*). Panel A shows the simulation over 9 ns, whereas panels B and C show the data for the two 3-ns simulations.

DISCUSSION

Generation of the model

The peptide

The starting model has been chosen with some arbitrary constraints, firstly the choice of the residues involved in the kink connecting helix-1 and helix-2 and the adopted angles of the resulting amide bonds for these residues. This bent structure has not been seen as the unique structural motif for the kink, but will hold as a plausible first trial on the investigations of the kink. Secondly, the helix-helix bend is undertaken in a direction so that the Ser-23 is not buried under helix-2. This arrangement is covered by the fact that Asp-39 and Arg-44 have been found experimentally (Henklein et al., 2000) to be aligned as shown in Fig. 3, graph on the left. Another plausible reason for the direction of the kink of helix-2 is that in a pentameric or hexameric assembly of the whole protein, Ser-23 would point into the putative pore. Helix-2 consists of a hydrophilic and hydrophobic ridge. In the current model the orientation of

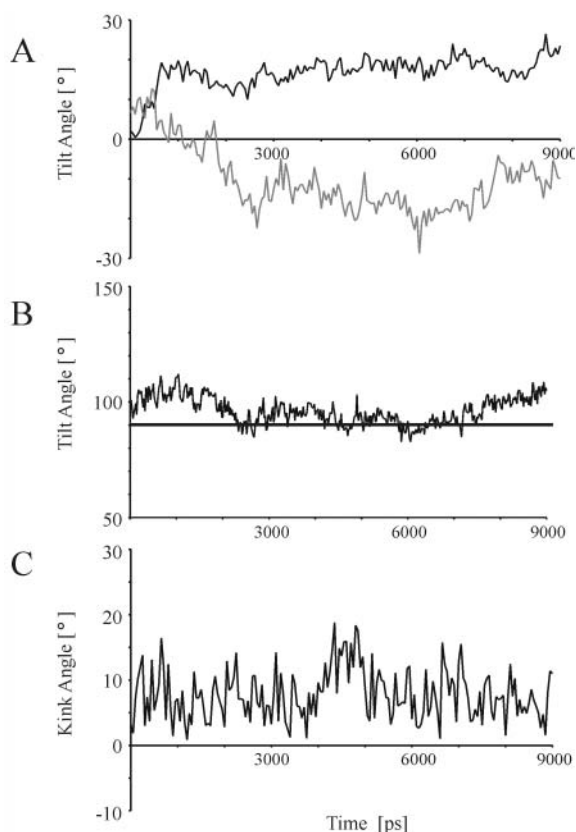


FIGURE 6 Evolution of the tilt angles of helix-1 (black trace) and helix-2 (gray trace) (A). Tilt angle between helix-1 and helix-2 is calculated from the cross product of the two vectors defined by the two helices: $\cos \alpha(t) = \mathbf{u}_1(t) \cdot \mathbf{u}_2(t)$; with \mathbf{u}_1 and \mathbf{u}_2 defining the vectors along the helix long axis of helix-1 and helix-2 (B). Kink angle for helix-1 (C).

helix-2 allows both ridges to face their favored environment: the hydrophilic side faces the aqueous phase whereas the hydrophobic side faces the hydrophobic slab of the bilayer. Thirdly, a tilt angle found experimentally for both helices in the starting structure is not adopted. It is expected that the experimentally proposed conformation represents a local minimum and that the simulation protocol would allow us to find this minimum if the starting structure would represent an energetically unfavorable conformation. Also tilt angles vary depending on the method (CD, solid-state NMR) and the laboratories, and may be determined by lipid thickness (Ridder et al., 2002).

The repeated simulation with different initial velocities results in almost identical structural features (e.g., Fig. 6). Thus, with this simulation protocol a relatively stable local minimum can be detected that allows then an interpretation of the data with more certainty. It also indicates to which extent the interpretation of events in a single simulation can be analyzed. A single simulation presents trends rather than absolute figures.

Another essential factor required for a proper analysis of the data is the length of the simulation. Interpretation of the

data obtained after 3 ns would result in the conclusion that the starting structure might be essential for the outcome. Because the peptide is moving out of the bilayer (Fig. 1 A), the appropriate starting structure might not have been chosen. Taking the full data set into account, the MD protocol adjusts for an unfavorable starting position. After 9 ns, independently of the starting structure used, the peptide embeds itself properly in the bilayer according to its hydrophobic shape. It cannot be ruled out that this overall translation parallel to the bilayer normal is as an oscillating movement on a longer timescale or a feature of the short timescales used (Fig. 1 A).

Although different starting velocities and one long simulation (9 ns) have been chosen, the outcome might not cover all conformational space involved in a stable local minimum characteristic for the bent. Future work also needs to address different geometrical starting structures with respect to the insertion of the peptide into the lipid bilayer and the kink, especially because MD simulations do not detect large conformational changes.

The lipid bilayer

A lipid bilayer with an uneven number of lipids has been used recently to characterize the properties of the KcsA ion channel (Shrivastava and Sansom, 2000). An uneven number of lipids on both sides of the bilayer reflects a frustrated system. In the current model the “vacuum” underneath helix-2 of Vpu causes the lipid tails to fill this space, which means there is a frustration in this section of the bilayer. In a dynamic system like a lipid bilayer it is also possible to a certain extent that the lipid tails of the opposing leaflet participate in filling up the space. Leaving the number of lipids equal on both sides would cause strong frustration on the level of the phospholipid headgroup region on the side of the leaflet containing helix-2. In both cases the frustrated system will possibly bias the peptide structure according to the different lateral pressure implemented (Zheng et al., 2001). In this study the first type of frustration has been chosen because such a system would allow the amphipathic helix-2 to settle at the lipid headgroup/lipid tail interface.

Calculation of the number of lipids per area (\AA^2) reveals similar values for both leaflets over the entire range of the simulation indicative of identical conditions on both sides within the time frame of the simulations.

A pK_A calculation of the starting structure at 0 ns reveals all titrable residues to be in their default ionization (charged) state (Sameer, Lemaitre, Jakobsson, and Fischer, data not shown) except for Glu-51, which should be partially charged. Calculations on the structure after 0.5 ns indicate that Glu-51 has reached a position stabilizing its ionized state. It needs to be stated that the ionization state might change throughout a complete simulation and would need a more frequent assessment in a simulation.

Comparison of experimental and computational data on the shape of Vpu and with other viral membrane proteins

To a certain extent, the data derived from the simulations here match with those from NMR experiments. The average tilt angle for the TM helix (helix-1) obtained in this study is $(23.3 \pm 2.1)^\circ$. This is within the range of data obtained in other simulation studies on helix-1 assembled parallel in homooligomeric bundles ($\sim 15^\circ$ (Cordes et al., 2002)) and also of those from NMR spectroscopy on truncated/full-length Vpu (Marassi et al., 1999; Wray et al., 1999). Consequently, the tilt angle seems to be independent of the rest of the protein and an intrinsic property of Vpu. Helix-2 does not hold its starting position. It rather undergoes an almost 90° revolution within the first 3 ns and remains in this position. One might speculate at this stage whether this discrepancy with experimental data (Henklein et al., 2000) is due to a long-lasting oscillating movement of helix-2 with respect to the time frame of the simulation and too short to be detected by NMR spectroscopy, which is anyway carried out in gel phase bilayer at low hydration (Henklein et al., 2000; Marassi et al., 2000). A reason for this could also be that the experimental data were taken with a truncated cytoplasmic peptide rather than with a peptide analogous to the one used in this study. According to the present data, the TM helix is stable up to Glu-29/Tyr-30. This matches the most recent results on an extended TM segment of Vpu reconstituted into micelles using H/D exchange studies in combination with solution NMR spectroscopy (Vpu₂₋₃₇ in Ma et al. (2002)), and is within the minimum range of a stable TM helix up to Val-25 proposed by MD simulations (Fischer et al., 2000). It is expected that the extent of helix-2 up to Ser-52 is due to the missing phosphorous group at this residue. According to results from NMR spectroscopy, this helix should be slightly shorter (Ma et al. 2002).

The shape of Vpu₁₋₅₂ with a TM helix and a second helix lying parallel to the lipid bilayer plane, is similar to that found for the viral coat proteins Pf1 (Azpiazu et al., 1993; Nambudripad et al., 1991; Shon et al., 1991), M13 (Glaubitz et al., 2000; Henry and Sykes, 1992; van der Ven et al., 1993; Wolkers et al., 1995) of filamentous bacteriophages, and most recently for phospholamban (Mascioni et al., 2002). Molecular dynamics simulations of Pf1 indicate that the helix residing on the membrane surface is rather strongly pointing with its N-terminal end into the bilayer (Roux and Woolf, 1996) compared to a more moderate tilt of $\sim 10^\circ$ for helix-2 in Vpu₁₋₅₂ pointing with the corresponding C-terminus toward the lipid bilayer. In contrast to the studies on Pf1, the C-terminal end of helix-2 in Vpu₁₋₅₂ is not as mobile as the corresponding N-terminal end in Pf1. Regarding the tilt angle of the TM helix, for Pf1 an angle of 30° is suggested in a Monte Carlo simulation upon the insertion process of Pf1 into the membrane (Milik and Skolnick, 1993) applying a mean-field potential to approximate the effect of the

membrane. The outcome of the simulations on Vpu₁₋₅₂ represents a common motif of helix alignment in a monotopic membrane protein with one helix traversing the lipid bilayer and the other helix lying parallel to the membrane surface (Turner and Weiner, 1993). Further simulations on Vpu with phosphorylated serines (Ser-52 and Ser-56) will be needed to address the effect of the phosphates on the alignment of helix-1 and the rest of the cytoplasmic part of Vpu in the simulations.

The data support the idea that the two helices are interconnected via a flexible linker, allowing the two helices to some extent to move independent from each other (see also Ma et al. (2002)). It might even be suggested that helix-1 has enough flexibility to form a putative channel via oligomerization with other proteins, and helix-2 fulfills its role as a “peptide float” riding on the bilayer separating helix-1 on the N-terminal side from the third helix (helix-3) and the rest of the protein toward the C-terminal side. The C-terminal side would then be able to dock to CD4, involving probably large mechanical movements, but without affecting helix-1. The results further implement the existence of “functional” modules present in Vpu. The idea of “functional” modules is an extension of the findings about proteins made up from modular repeated “building” blocks (Campbell and Downing, 1998; Doolittle, 1995). No larger repeat units of this type are found and would be necessary for constructing the whole protein (building modules). The protein is simply too short, but each structural unit has its essential functional role (functional modules).

The EYR motif

From the simulations it can be concluded that the first residues involved in the EYR motif retain a reasonable helical motif. According to the conformation, i), Glu-28 is further able to support the loop via the formation of salt bridges with Lys-31 and Arg-34; ii), Tyr-29 can anchor the protein within the lipid bilayer (de Planque et al., 2002; Ulmschneider and Sansom, 2001); and iii), Arg-30 is free to point into a pore and function as a putative selectivity filter. Residues involved in the connection of the two helices by forming a loop are the following residues Lys-31 to Arg-34. Salt bridge formation of Lys-31 with Glu-38 and Arg-34 stabilize the loop. A similar role of causing a kink in connection with a loop is attributed to a close location of a Lys-20 to Asp-18 in the viral coat protein Pf1 (Tobias et al., 1993).

Modeled structures demand the validation of the data and to which extent information can be deduced from them. With a single MD simulation, structural features can be resolved, however, even with repeated simulations the data have to be “smoothed” by the interpreter. The results regarding the salt bridges (Fig. 5) would indicate from Fig. 5 A, that the salt bridge Glu-28–Lys-31 is constantly formed over the first

3 ns. Fig. 5, *B* and *C*, show that, also within the first 3 ns, some rupture might occur. Compared to the results from salt bridge Glu-28–Arg-34, and in light of the repeated simulations, the statement should be such that the formation of the salt bridge settles faster for Glu-28–Lys-31 within the first 3 ns.

Future studies need to address more conformational space regarding initial starting structures to suggest structural motifs involved in protein function. Also lipid frustration and its effect on protein structure in an all-atom simulation has to be explored in more detail.

CONCLUSION

The study supports that flexible parts are essential to connect units with specific functional roles and Vpu is consequently built of “functional modules.” This allows for structural features such as, e.g., the tilt angle of helix-1 independent of the rest of the protein. Helix-2 might form a “peptide float” riding on top of the bilayer. It is also concluded, as a consequence of the simulations on the individual modules, that it is possible to yield meaningful results representative for the whole protein.

Vpu uses an internal salt bridge formation involving three residues to connect helix-1 with helix-2 and to orient the second helix on top of the bilayer. The EYR motif seems to be an important motif involved in confining the conformation of Vpu.

We thank P. Tieleman (Calgary, Canada) for providing us with an equilibrated lipid membrane and thanks to S. Grage (Oxford) for interesting discussions.

The Engineering and Physical Sciences Research Council (EPSRC) is acknowledged for financial support (to A.W.). The Biotechnology and Biological Sciences Research Council (BBSRC) is acknowledged for a Professional Research Fellowship (to A.W.) and grant support.

REFERENCES

- Azpiazua, I., J. C. Gomez-Fernandez, and D. Chapman. 1993. Biophysical studies of the Pf1 coat protein in the filamentous phage, in detergent micelles, and in a membrane environment. *Biochemistry*. 32:10720–10726.
- Barlow, D., and J. Thornton. 1988. Helix geometry in proteins. *J. Mol. Biol.* 201:601–619.
- Berendsen, H. J. C., J. R. Grigera, and T. P. Straatsma. 1987. *J. Phys. Chem.* 91:6269–6271.
- Boncheva, M., and H. Vogel. 1997. Formation of stable polypeptide monolayers at interfaces: controlling molecular conformation and orientation. *Biophys. J.* 73:1056–1072.
- Bour, S., U. Schubert, and K. Strebel. 1995. The human immunodeficiency virus type 1 Vpu protein specifically binds to the cytoplasmic domain of CD4: implications for the mechanism of degradation. *J. Virol.* 69:1510–1520.
- Branden, C., and J. Tooze. 1991. Introduction to Protein Structure. Garland, New York.
- Brünger, A. T. 1992. X-PLOR Version 3.1. A System for X-ray Crystallography and NMR. Yale University Press, New Haven.
- Campbell, I. D., and A. K. Downing. 1998. NMR of modular proteins. *Nat. Struct. Biol. Suppl.* 496–499.
- Coadou, G., N. Evrard-Todeschi, J. Gharbi-Benarous, R. Benarous, and J.-P. Girault. 2001. Conformational analysis by NMR and molecular modelling of the 41–62 hydrophilic region of HIV-1 encoded virus protein U (Vpu). Effect of the phosphorylation on sites 52 and 56. *C. R. Acad. Sci. Paris, Chemie/Chemistry*. 4:751–758.
- Cohen, E. A., E. F. Terwilliger, J. G. Sodroski, and W. A. Haseltine. 1988. Identification of a protein encoded by the *vpu* gene of HIV-1. *Nature*. 334:532–534.
- Cordes, F., A. Kukol, L. R. Forrest, I. T. Arkin, M. S. P. Sansom, and W. B. Fischer. 2001. The structure of the HIV-1 Vpu ion channel: modelling and simulation studies. *Biochim. Biophys. Acta.* 1512:291–298.
- Cordes, F. S., A. Tustian, M. S. P. Sansom, A. Watts, and W. B. Fischer. 2002. Bundles consisting of extended transmembrane segments of Vpu from HIV-1: computer simulations and conductance measurements. *Biochemistry*. 41:7359–7365.
- de Planque, M. R. R., J.-W. P. Boots, D. T. S. Rijkers, R. M. J. Liskamp, D. V. Greathouse, and J. A. Killian. 2002. The effect of hydrophobic mismatch between phosphatidylcholine bilayers and transmembrane α -helical peptides depend on the nature of interfacially exposed aromatic and charged residues. *Biochemistry*. 41:8396–8404.
- Deisenhofer, J., O. Epp, K. Miki, R. Huber, and H. Michel. 1985. Structure of the protein subunits in the photosynthetic reaction centre of *Rhodospseudomonas viridis* at 3 Å resolution. *Nature*. 318:618–624.
- Deora, A., P. Spearman, and L. Ratner. 2000. The N-terminal matrix domain of HIV-1 Gag is sufficient but not necessary for viral protein U-mediated enhancement of particle release through a membrane-targeting mechanism. *Virology*. 269:305–312.
- Doolittle, R. F. 1995. The multiplicity of domains in proteins. *Annu. Rev. Biochem.* 64:287–314.
- Ewart, G. D., T. Sutherland, P. W. Gage, and G. B. Cox. 1996. The Vpu protein of human immunodeficiency virus type 1 forms cation-selective ion channels. *J. Virol.* 70:7108–7115.
- Faraldo-Gomez, J. D., G. R. Smith, and M. S. P. Sansom. 2002. Setting up and optimization of membrane protein simulations. *Eur. Biophys. J.* 31:217–227.
- Federau T., U. Schubert, J. Floßdorf, P. Henklein, D. Schomburg, and V. Wray. 1996. Solution structure of the cytoplasmic domain of the human immunodeficiency virus type 1 encoded virus protein U (Vpu). *Int. J. Peptide Protein Res.* 47:297–310.
- Fischer, W. B., L. R. Forrest, G. R. Smith, and M. S. P. Sansom. 2000. Transmembrane domains of viral ion channel proteins: a molecular dynamics simulation study. *Biopolymers*. 53:529–538.
- Fischer, W. B., and M. S. P. Sansom. 2002. Viral ion channels: structure and function. *Biochim. Biophys. Acta.* 1561:27–45.
- Glaubitz, C., G. Gröbner, and A. Watts. 2000. Structural and orientational information of the membrane embedded M13 coat protein by ^{13}C -MAS NMR spectroscopy. *Biochim. Biophys. Acta.* 1463:151–161.
- Grice, A. L., I. D. Kerr, and M. S. P. Sansom. 1997. Ion channels formed by HIV-1 Vpu: a modelling and simulation study. *FEBS Lett.* 405:299–304.
- Hendsch, Z. S., and B. Tidor. 1994. Do salt bridges stabilize proteins? A continuum electrostatic analysis. *Protein Sci.* 3:211–226.
- Henklein, P., R. Kinder, U. Schubert, and B. Bechinger. 2000. Membrane interactions and alignment of structures within the HIV-1 Vpu cytoplasmic domain: effect of phosphorylation of serines 52 and 56. *FEBS Lett.* 482:220–224.
- Henry, G. D., and B. D. Sykes. 1992. Assignment of amide ^1H and ^{15}N NMR resonances in detergent-solubilized M13 coat protein: a model for the coat protein dimer. *Biochemistry*. 31:5284–5297.
- Horowitz, A., L. Serrano, B. Avron, M. Bycroft, and A. R. Fersht. 1990. Strength and co-operativity of contributions of salt bridges to protein stability. *J. Mol. Biol.* 216:1031–1044.
- Kerr, I. D., R. Sankaramakrishnan, O. S. Smart, and M. S. P. Sansom. 1994. Parallel helix bundles and ion channels: molecular modeling via simulated annealing and restrained molecular dynamics. *Biophys. J.* 67: 1501–1515.

- Kukul, A., and I. T. Arkin. 1999. Vpu transmembrane peptide structure obtained by site-specific fourier transform infrared dichroism and global molecular dynamics searching. *Biophys. J.* 77:1594–1601.
- Lopez, C. F., M. Montal, J. K. Blasie, M. L. Klein, and P. B. Moore. 2002. Molecular dynamics investigation of membrane-bound bundles of the channel-forming transmembrane domain of viral protein U from the Human Immunodeficiency Virus HIV-1. *Biophys. J.* 83:1259–1267.
- Ma, C., F. M. Marassi, D. H. Jones, S. K. Straus, S. Bour, K. Strebel, U. Schubert, M. Oblatt-Montal, M. Montal, and S. J. Opella. 2002. Expression, purification, and activities of full-length and truncated versions of the integral membrane protein Vpu from HIV-1. *Protein Sci.* 11:546–557.
- Marassi, F. M., C. Ma, J. J. Gesell, and S. J. Opella. 2000. Three-dimensional solid-state NMR spectroscopy is essential for resolution of resonance from in-plane residues in uniformly ^{15}N -labeled helical membrane proteins in oriented lipid bilayers. *J. Magn. Res.* 144:156–161.
- Marassi, F. M., C. Ma, H. Gratkowski, S. K. Straus, K. Strebel, M. Oblatt-Montal, M. Montal, and S. J. Opella. 1999. Correlation of the structural and functional domains in the membrane protein Vpu from HIV-1. *Proc. Natl. Acad. Sci. USA.* 96:14336–14341.
- Marqusee, S., and R. L. Baldwin. 1987. Helix stabilization by $\text{Glu}^- \dots \text{Lys}^+$ salt bridges in short peptides of *de novo* design. *Proc. Natl. Acad. Sci. USA.* 84:8898–8902.
- Mascioni, A., C. Karim, J. Zmoon, D. D. Thomas, and G. Veglia. 2002. Solid-state NMR and rigid body molecular dynamics to determine domain orientations of monomeric phospholamban. *J. Am. Chem. Soc.* 124:9392–9393.
- Milik, M., and J. Skolnick. 1993. Insertion of peptide chains into lipid membranes: an off-lattice Monte Carlo dynamics model. *Proteins.* 15:10–25.
- Moore, P. B., Q. Zhong, T. Husslein, and M. L. Klein. 1998. Simulation of the HIV-1 Vpu transmembrane domain as a pentameric bundle. *FEBS Lett.* 431:143–148.
- Musafia, B., V. Buchner, and D. Arad. 1995. Complex salt bridges in proteins: statistical analysis of structure and function. *J. Mol. Biol.* 254:761–770.
- Nambudripad, R., W. Stark, S. J. Opella, and L. Makowski. 1991. Membrane-mediated assembly of filamentous bacteriophage Pf1 coat protein. *Science.* 252:1305–1308.
- Paul, M., S. Mazumder, N. Raja, and M. Abdul Jabbar. 1998. Mutational analysis of the human immunodeficiency virus type 1 Vpu transmembrane domain that promotes the enhanced release of virus-like particles from the plasma membrane of mammalian cells. *J. Virol.* 72:1270–1279.
- Ridder, A. N. J. A., W. van de Hoef, J. Stam, A. Kuhn, B. de Kruijff, and J. A. Killian. 2002. Importance of hydrophobic matching for spontaneous insertion of a single-spanning membrane protein. *Biochemistry.* 41:4946–4952.
- Roux, B., and T. B. Woolf. 1996. Molecular dynamics of Pf1 coat protein in a phospholipid bilayer. In *Biological Membranes*, K. M. Merz, Jr. and B. Roux, editors. Birkhäuser, Boston. 555–587.
- Sansom, M. S. P., I. H. Shrivastava, J. N. Bright, J. Tate, C. E. Capener, and P. C. Biggin. 2002. Potassium channels: structures, models, simulations. *Biochim. Biophys. Acta.* 1565:294–307.
- Schubert, U., S. Bour, A. V. Ferrer-Montiel, M. Montal, F. Maldarelli, and K. Strebel. 1996a. The two biological activities of human immunodeficiency virus type 1 Vpu protein involve two separable structural domains. *J. Virol.* 70:809–819.
- Schubert, U., A. V. Ferrer-Montiel, M. Oblatt-Montal, P. Henklein, K. Strebel, and M. Montal. 1996b. Identification of an ion channel activity of the Vpu transmembrane domain and its involvement in the regulation of virus release from HIV-1-infected cells. *FEBS Lett.* 398:12–18.
- Shon, K.-J., Y. Kim, L. A. Colnago, and S. J. Opella. 1991. NMR studies of the structure and dynamics of membrane-bound bacteriophage Pf1 coat protein. *Science.* 252:1303–1305.
- Shrivastava, I. H., and M. S. P. Sansom. 2000. Simulations of ion permeation through a potassium channel: molecular dynamics of KcsA in a phospholipid bilayer. *Biophys. J.* 78:557–570.
- Strebel, K., T. Klimkait, F. Maldarelli, and M. A. Martin. 1989. Molecular and biochemical analysis of human deficiency virus type 1 vpu protein. *J. Virol.* 63:3784–3791.
- Strebel, K., T. Klimkait, and M. A. Martin. 1988. Novel gene of HIV-1, vpu, and its 16-kilodalton product. *Science.* 241:1221–1223.
- Tiganos, E., J. Friberg, B. Allain, N. G. Daniel, X.-J. Yao, and E. A. Cohen. 1998. Structural and functional analysis of the membrane-spanning domain of the Human Immunodeficiency Virus Type 1 Vpu protein. *Virology.* 251:96–107.
- Tobias, D. J., M. L. Klein, and S. J. Opella. 1993. Molecular dynamics simulation of Pf1 coat protein. *Biophys. J.* 64:670–675.
- Turner, R. J., and J. H. Weiner. 1993. Evaluation of transmembrane helix prediction methods using the recently defined NMR structures of the coat proteins from bacteriophages M13 and Pf1. *Biochim. Biophys. Acta.* 1202:161–168.
- Ulmschneider, M., and M. S. P. Sansom. 2001. Amino acid distribution in integral membrane protein structures. *Biochim. Biophys. Acta.* 1512:1–14.
- van der Ven, F. J. M., J. W. M. van Os, J. M. A. Aelen, S. S. Wymenga, M. L. Remerowski, R. N. H. Konings, and C. W. Hilbers. 1993. Assignment of ^1H , ^{15}N , and backbone ^{13}C resonances in detergent-solubilized M13 coat protein via multinuclear multidimensional NMR: a model for the coat protein monomer. *Biochemistry.* 32:8322–8328.
- van Gunsteren, W. F., and A. E. Mark. 1998. Validation of molecular dynamics simulation. *J. Chem. Phys.* 108:6109–6116.
- Waldburger, C. D., J. F. Schildbach, and R. T. Sauer. 1995. Are buried salt bridges important for protein stability and conformational specificity? *Nat. Struct. Biol.* 2:122–128.
- Willbold, D., S. Hoffmann, and P. Rösch. 1997. Secondary structure and tertiary fold of the human immunodeficiency virus protein U (Vpu) cytoplasmic domain in solution. *Eur. J. Biochem.* 245:581–588.
- Willey, R. L., F. Maldarelli, M. A. Martin, and K. Strebel. 1992. Human immunodeficiency virus type 1 Vpu protein induces rapid degradation of CD4. *J. Virol.* 66:7193–7200.
- Wolkers, W. F., P. I. Haris, A. M. A. Pistorius, D. Chapman, and M. A. Hemminga. 1995. FT-IR spectroscopy of the major coat protein of M13 and Pf1 in the phage and reconstituted into phospholipid systems. *Biochemistry.* 34:7825–7833.
- Wray, V., T. Federau, P. Henklein, S. Klabunde, O. Kunert, D. Schomburg, and U. Schubert. 1995. Solution structure of the hydrophilic region of HIV-1 encoded virus protein U (Vpu) by CD and ^1H NMR-spectroscopy. *Int. J. Pept. Protein Res.* 45:35–43.
- Wray, V., R. Kinder, T. Federau, P. Henklein, B. Bechinger, and U. Schubert. 1999. Solution structure and orientation of the transmembrane anchor domain of the HIV-1-encoded virus protein U by high resolution and solid-state NMR spectroscopy. *Biochemistry.* 38:5272–5282.
- Zheng, S., J. Strzalka, C. Ma, S. J. Opella, B. M. Ocko, and J. K. Blasie. 2001. Structural studies of the HIV-1 accessory protein Vpu in Langmuir monolayers: synchrotron x-ray reflectivity. *Biophys. J.* 80:1837–1850.